Table 2.1: Parameters that influence the braking distance. Classification in the time domain and in the domain of controllability.

	Measurable and Controllable	**Only Measurable**	**Neither Measur- nor Controllable**
Short Run	• Time at which the clutch is uncoupled t_{C} • Settings of the active shock absorbers I_{D} • Course of wheel load	• Course of steering wheel angle • Actions of the ABS-controller $p_{\mathrm{ABS},i}$	• Variations of local friction factor μ
Medium-term Run	• Initial velocity $v_{\mathrm{x},0}$ • Tire temperature T_{T}[8] • Gradient of braking pressure at the beginning of the braking procedure • Braking disc temperature T_{B}[9] • Slope of the road • Gear in which a braking procedure is executed	• Wind direction • Wind speed	
Long Run	• Tire inflation pressure p_{T}	• Surrounding air pressure • Surrounding air density • Road condition (dry, wet) • Type of road (cobblestone, asphalt, ...) • Pavement temperature t_{P}	• Vehicle's mass distribution

And an example for a quantity that can neither be measured nor controlled is the actual local friction coefficient between tire and pavement.

Other parameters, such as the drag coefficient, are assumed to be constant for all times. Though they have an influence on the absolute value of the braking distance, they do not vary and therefore do not influence the braking distance differently from one braking procedure to another.

In the experimental setup for full-braking tests all those parameters that can be controlled are kept constant. The other parameters influence the braking distance in a stochastic way. Their influence cannot be eliminated, thus they must be treated statistically by using methods of statistics.

2.3 Possibilities to Influence the Braking Force

In Figure 2.7 forces and torques at a spinning, braked wheel are shown. In the following the quantities used shall be introduced and defined.

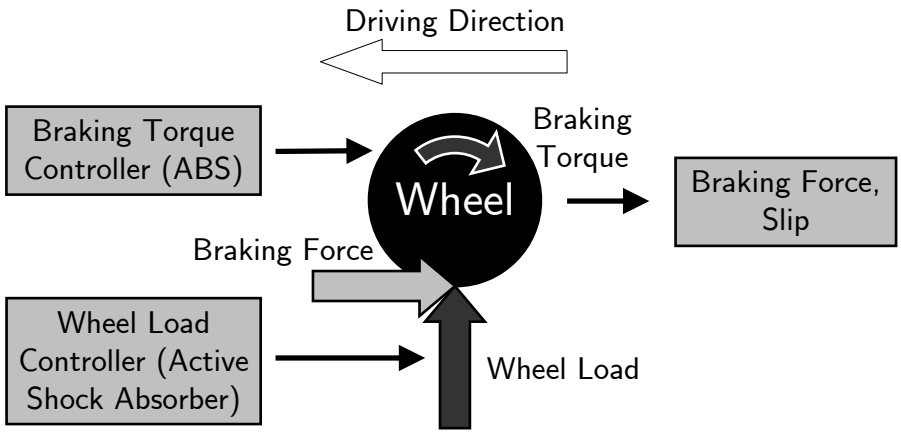

Figure 2.7: Possibilities to influence the braking force by either a braking torque or a wheel-load controller. As for the braking torque controller the ABS is state-of-the-art, as for the wheel-load controller active shock absorbers are used in this thesis.

Braking Force F_{B}

The braking force at a wheel is the longitudinal part of the tire force in the contact zone of tire and pavement. The braking force causes the vehicle to decelerate and the wheel at which it is applied to accelerate.

Braking Torque M_{B}

The braking torque at a wheel is the torque around the wheel's y-axis that causes the wheel to decelerate.

Braking Slip λ_{B}

The braking slip at a wheel is defined as the difference of vehicle's longitudinal speed v_{x} and wheel speed v_{W} per v_{x}. If the wheel locks, the braking slip equals one. If the wheel is

completely free spinning, the braking slip equals zero.

$$\lambda_{\mathrm{B}}(t) = \frac{v_{\mathrm{x}}(t) - v_{\mathrm{W}}(t)}{v_{\mathrm{x}}(t)} = 1 - \frac{\omega_{\mathrm{W}}(t)\, r_{\mathrm{eff}}}{v_{\mathrm{x}}(t)} \tag{2.27}$$

Braking Coefficient μ

The braking coefficient μ at a wheel is defined as ratio of braking force F_{B} at the wheel and wheel load F_{z} at the same wheel (for the definition of wheel load refer to section 4.1). Its maximum value μ_{max} is reached if at a given level of wheel load the braking force cannot be increased anymore.

$$\mu(t) = \frac{F_{\mathrm{B}}(t)}{F_{\mathrm{z}}(t)} \tag{2.28}$$

$$\mu_{\mathrm{max}} = \left.\frac{F_{\mathrm{B,max}}}{F_{\mathrm{z}}}\right|_{F_{\mathrm{z}}=\mathrm{const.}} \tag{2.29}$$

Applying the principle of angular momentum to the spinning wheel leads to:

$$J_{\mathrm{W}}\, \ddot{\varphi}_{\mathrm{W}}(t) = F_{\mathrm{B}}(t)\, r_{\mathrm{eff}} - M_{\mathrm{B}}(t), \tag{2.30}$$

where J_{W} is the mass moment of inertia of the wheel, $\ddot{\varphi}_{\mathrm{W}}$ is the angular acceleration of the wheel, and r_{eff} is the wheel's effective radius. The braking force and the wheel load are connected via equation 2.28, where μ again is a function of the braking slip λ_{B}.

$$\mu = \mu(\lambda_{\mathrm{B}}) \tag{2.31}$$

The braking slip is defined in equation 2.27. In its definition the rotational speed of the wheel is involved, which means that the loop is closed back to equation 2.30.

From those simple considerations it becomes clear that the angular dynamics of the wheel and with it the dynamics of the braking force have two inputs: Braking torque and wheel load. Even though there are several parameters which do influence the braking performance via their influence on the braking force (refer to section 2.2.2), generally speaking there are those two parameters to influence the braking force on a braked wheel which can be controlled by a car-internal system. The braking force can either be manipulated by controlling the braking torque or by controlling the wheel load. Both are inputs for the wheel-system. Their values together with other uncontrollable parameters determine the braking slip and the braking force.

If there is a braking torque applied to a wheel, the wheel will slow down. This means that then the wheel spins slower than it ought to spin in order to hold the same longitudinal speed as the vehicle does. The slowing down of the wheel together with the constant longitudinal velocity of the vehicle leads to a braking slip at the wheel. This means that in the tire contact area there are longitudinal forces acting between pavement and tire, because there is a gap in speeds of vehicle and wheel/tire.

A slipping wheel is slightly different from standard rubber friction. In the case of standard rubber friction as it is shown in Figure 2.8, two main processes lead to a friction force: hysteresis and adhesion. While hysteresis is due to the unevenness of the pavement

and is therefore only effected little by changing friction coefficient of the pavement-tire-connection, adhesion strongly depends on this friction coefficient. Adhesion is therefore much smaller for wet roads than for dry ones, while hysteresis is almost not effected by such changes. Both effects need little amounts of deformation of the rubber in longitudinal direction to have an effect.

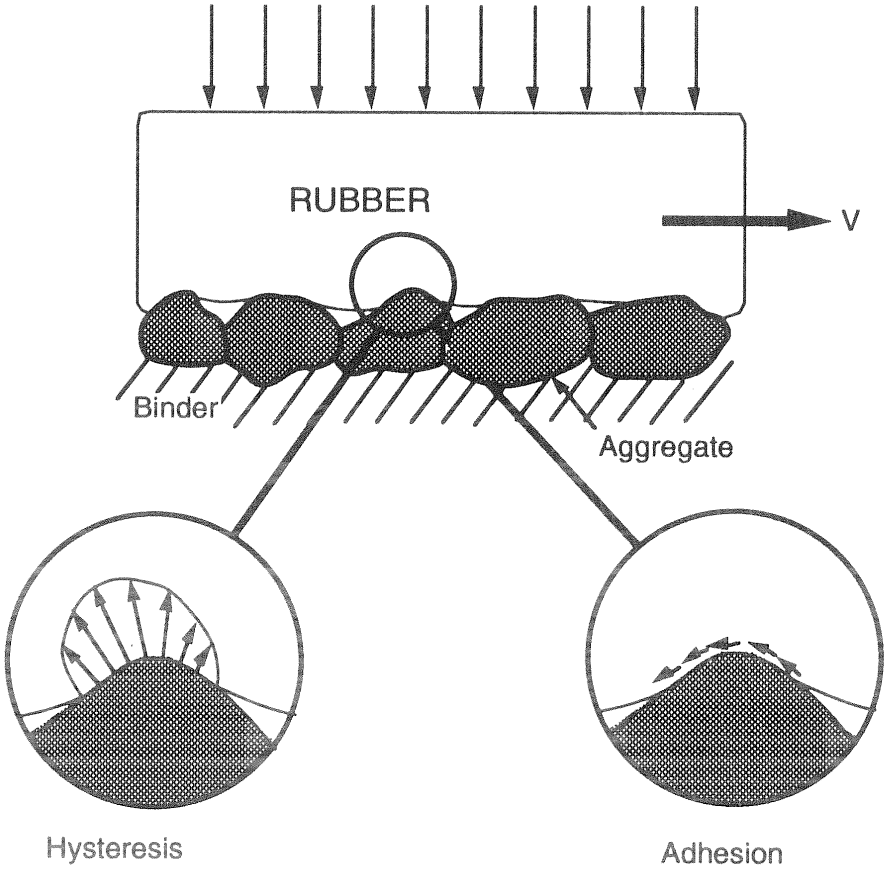

Figure 2.8: Mechanisms of rubber friction[10].

Anyways, if the maximum applicable friction coefficient is exceeded, the rubber in Figure 2.8 begins to slide. The same holds true in case of a spinning tire with braking torque applied.

The difference is that the total tire contact zone can be divided into different contact areas, and depending on the amount of braking torque applied more or less of those areas have slipping tread elements. A tread element at the very beginning of the contact zone is undeformed. As it enters the contact zone it gets deformed. This deformation is caused by the friction force between pavement and tire. The friction force again occurs because there is a velocity difference of the tread elements of the tire and the pavement, which is caused by the deceleration of the wheel due to the braking torque applied. The further the tread element goes to the center of the tire contact zone the more deformation is applied to it.

[10]cp. Meyer/Kummer (1962): Mechanism of force transmission between tire and road p. 18 according to Gillespie (1992): Fundamentals of Vehicle Dynamics p. 54

At high braking levels there are areas of the total contact zone in which the adhesion forces of the tread element cannot stand the deformation anymore and the respective elements begin to slip. In those areas the friction force is decreasing.

Figure 2.9 shows the described process. The vertical load, the friction force, and the relative slip are shown. The integrals over the total tire contact zone of those three quantities give the total wheel load, the total braking force, and the total braking slip of the wheel. Therefore, the whole deformation and relaxation process finally leads to the braking force of the wheel that leads to the deceleration of the vehicle.

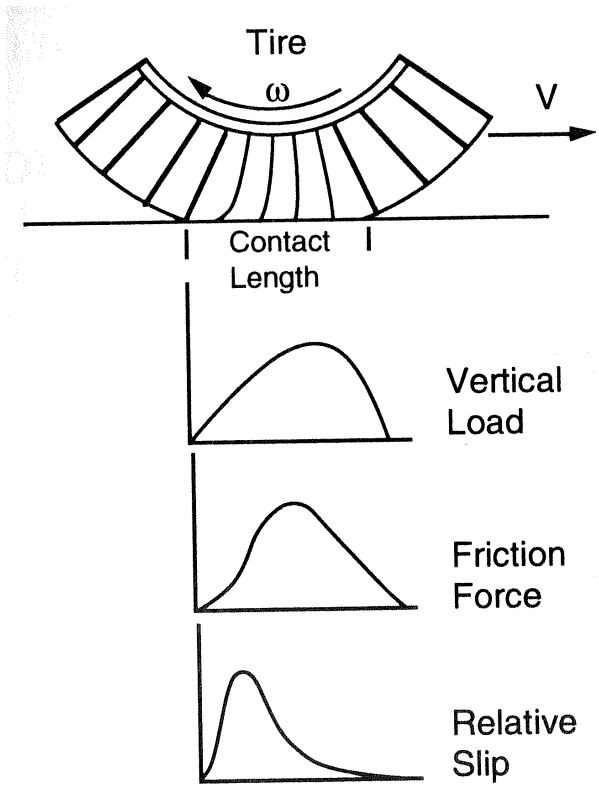

Figure 2.9: Deformation of the tire in its contact zone due to braking torque and braking force applied in a braking situation[11].

It also becomes clear that if and only if a braking slip occurs a braking force can be applied to the ground. Furthermore, the maximum braking force is applied at braking slip levels in the lower part of the spectrum from zero to one and not if the wheel locks. In this locked case every single tread element slides over the ground. Since friction forces are greater for friction of rest than for sliding friction, the maximum braking force applicable is the greater the less contact areas do slide.

In the best case (maximum braking force) the tread elements are all close to sliding but do not totally slide and sliding is limited to local areas. The reasoning given also explains why for bold tires the optimal braking slip is lower than for brand-new tires. The shorter the deformable tread elements, the stiffer they are. This means that the same amount of longitudinal force causes less deformation. Also the maximum braking force just before the tread element slips is reached at lower deformation levels. That is why the braking slip has smaller values the shorter the tread elements are.

[11] Gillespie (1992): Fundamentals of Vehicle Dynamics p. 55

2.3.1 Influence via Braking Torque—ABS

The braking torque—which is the reason for the deceleration of the wheel and the existence of the braking force—can be applied to a wheel in several different ways, e. g. by electromagnetic forces or by frictional forces. In any case the braking torque times the angular velocity of the wheel delivers the part of total braking power at a wheel that is converted by the brake. The other part of the total braking power is converted in the tire contact zone. This part is calculated by the velocity difference of longitudinal velocity v_x and wheel speed $v_W = \omega_W r_{eff}$ times the braking force at the respective wheel.

The ratio of the part of the total braking power converted in the tire contact zone and the total braking power itself equals the braking slip. In case of a locked wheel, i. e. 100 % braking slip, the entire braking power is converted in the tire-pavement-zone.

In case that the braking torque is applied by a frictional force, the frictional partners (e. g. braking disc and braking pads) have to be compressed by a normal force. This normal force together with the actual friction coefficient leads to the actual friction force. The normal force again can be generated in different ways, e. g. hydraulically, mechanically, or pneumatically. In today's series passenger cars the hydraulic solution predominates all other solutions by far.

Figure 2.10 shows the principle layout of an Antilock Braking System (ABS) within a hydraulic braking system. The force applied by the driver at the braking pedal increases the braking pressure in the brake master cylinder (BMC). This pressure is transmitted via the brake lines to the wheel-brake cylinders. If the pressure applied by the driver is low, the ABS will not control, the vehicle brakes as if the ABS was not there. This means the inlet valves are opened, the outlet valves at every wheel are closed.

If the braking slip at a wheel becomes too large, the respective inlet valve is closed in order to disconnect the BMC and the high pressure from the respective wheel-brake cylinder. If the slip is still too large or is even increasing, the outlet valve is opened. By this the braking pressure at the critical wheel is released and with it the braking torque. The ABS therefore has three possible settings for every wheel: inlet valve open and outlet valve closed, inlet valve closed and outlet valve closed, inlet valve closed and outlet valve opened. The variable $p_{ABS,i}$ is introduced, which can take values of -1, 0, and +1, depending on the ABS' current action at the i-th wheel. These three settings shall be named as:

- Increase braking pressure = inlet valve opened and outlet valve closed: $p_{ABS} = +1$
- Hold braking pressure = inlet valve closed and outlet valve closed: $p_{ABS} = 0$
- Release braking pressure = inlet valve closed and outlet valve opened: $p_{ABS} = -1$

The ABS implemented in the testing vehicle also works on the hydraulic basis with a system similar to the one shown in Figure 2.10. The signals of the wheel-speed sensors are used to calculate the actual velocity v_x of the car and to decide if one of the wheels is about to lock or not.

The algorithm of deciding between increasing, holding, or decreasing braking pressure is shown in Figure 2.11. It shows a control cycle of a today's ABS for high friction conditions (friction between pavement and tire). The increase of braking pressure leads to a decreasing velocity v_x and an also decreasing angular velocity ω_W of the wheel.

[12] Robert Bosch GmbH (1999): Kraftfahrtechnisches Taschenbuch p. 665

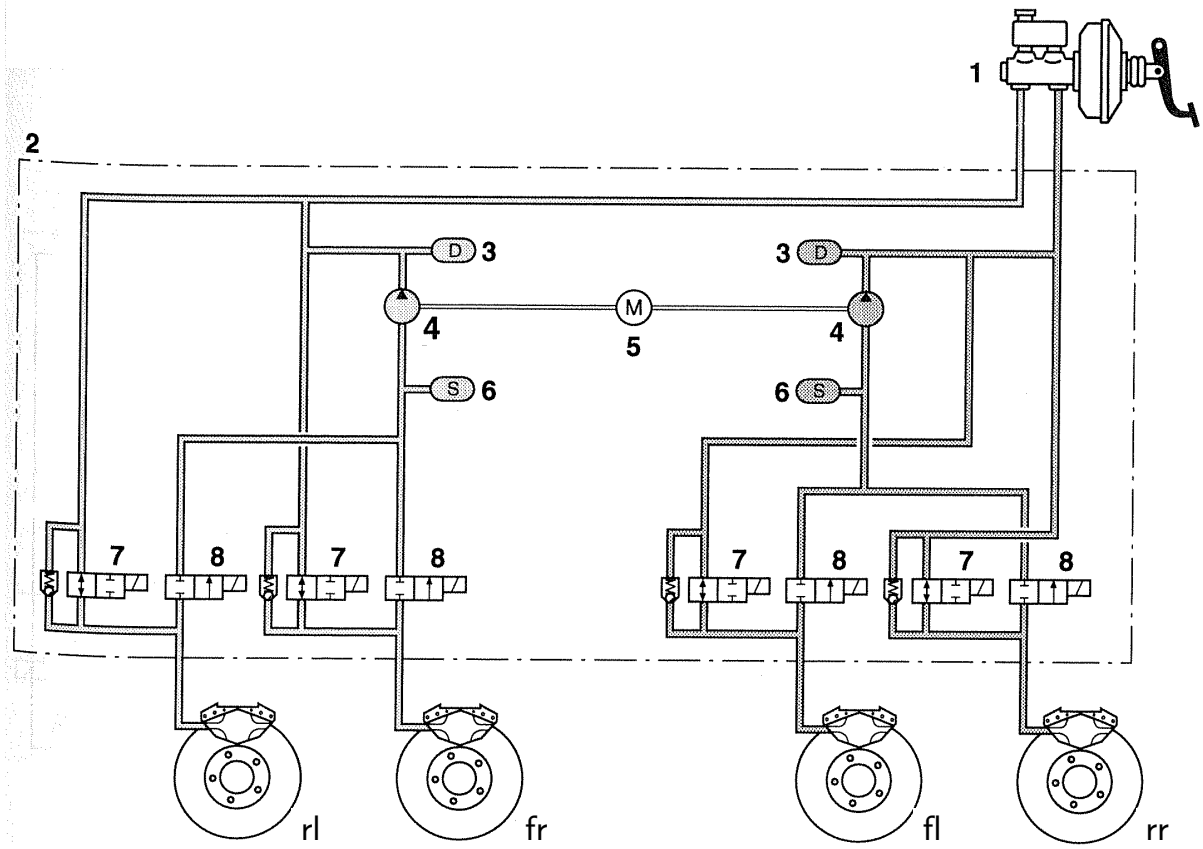

Figure 2.10: Setup of an Antilock Braking System (ABS) that is similar to the one installed in the testing vehicle[12]. 1: Brake master cylinder (BMC), 2: Hydraulic unit, 3: Damping chamber, 4: Return pump, 5: Motor, 6: Reservoir, 7: Inlet valves, 8: Outlet valves.

The angular acceleration of the wheel $\dot{\omega}_{\mathrm{W}}$ is negative and stays at a more or less constant level while the braking force and therefore the braking slip is increasing. If the maximum of the μ-slip curve is reached (refer to Figure 2.5), $\dot{\omega}_{\mathrm{W}}$ drops dramatically. This happens because at the maximum of the μ-slip curve a further increase in braking torque cannot be compensated by an increase in braking force anymore. It must therefore lead to an angular acceleration of the wheel which will finally make it lock—if the braking pressure and with it the braking torque is not lowered in time. This sudden drop of wheel angular acceleration is detected by the ABS. Once the threshold $(-a)$ is passed, the braking pressure is kept constant (hold braking pressure). The wheel speed at the time of passing the threshold a is memorized and named $v_{\mathrm{reference}}$. Due to the negative angular acceleration of the wheel, the wheel speed will also drop. If the wheel speed referred to $v_{\mathrm{reference}}$ drops below a slip threshold λ_1, the braking pressure is released ($p_{\mathrm{ABS}} = -1$), in order to prevent the wheel to lock and to keep the braking slip close to the optimal braking slip with the highest friction coefficient possible.

An important point to keep in mind is that, due to the ignorance of the ABS about the type of tire used, the ABS needs to determine where the optimal braking slip lies for every braking process newly. Thus, the first drop in wheel angular acceleration and in wheel speed can never be prevented. It is rather a necessary part of the ABS control algorithm.

This first drop in angular acceleration happens shortly before the maximum of the μ-slip curve is reached. Because of the degressiv curvature of the μ-slip curve close to its maximum, an increase in braking torque does not lead to an increase in braking force in the same dimension anymore—this is what happens in the linear part of the μ-slip curve. Hence, because the ABS waits for the angular acceleration to drop below the threshold $(-a)$ and the first drop happens close to the maximum of the μ-slip curve, this waiting can be treated as determining the maximum of the μ-slip curve[13].

Due to releasing the braking pressure, the angular acceleration of the wheel will increase again. Once it crosses the threshold $(-a)$—this time from below—, the braking pressure is kept constant again. If this constant level of braking pressure is such low that the wheel will spin up more and more, the braking pressure can be increased again. This happens if the angular acceleration of the wheel crosses the threshold A. If this very threshold is crossed from above again, the braking pressure is kept constant. It increases even further once $\dot{\omega}_{\mathrm{W}}$ crosses the threshold $+a$. Then the control cycle starts from its beginning. The whole process is meant to find the optimal braking slip and to adjust the actual braking slip to it.

[13]Robert Bosch GmbH (1999): Kraftfahrtechnisches Taschenbuch p. 662.
[14]Robert Bosch GmbH (2000): Automotive Handbook p. 662

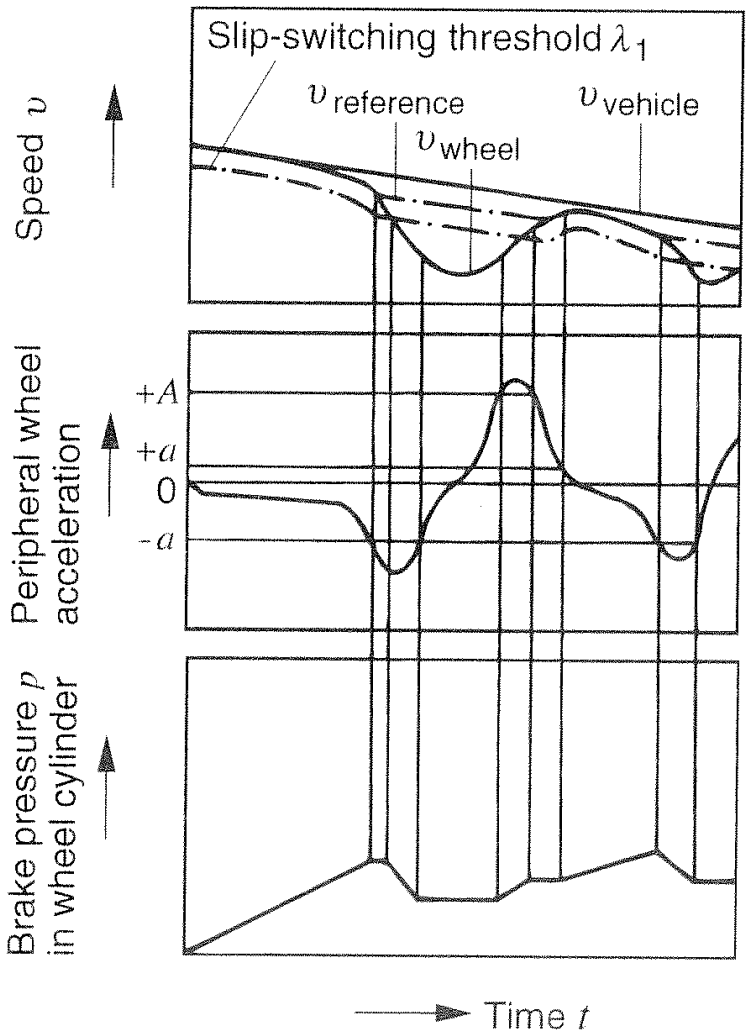

Figure 2.11: ABS control cycle for large friction coefficients[14]. $v_{\text{wheel}} = v_{\text{W}}$, $v_{\text{vehicle}} = v_{\text{x}}$.

2.3.2 Influence via Wheel Load—Active Shock Absorbers

For two reasons the ABS cannot completely reach the goal of keeping the braking slip constant at the optimal level: Firstly, information about the actual μ-slip curve is not present. The ABS has to estimate it. Secondly, and this is even more limiting, the ABS has no influence on the vertical tire force: the wheel load. But this force is the second input for the angular dynamics of the wheel (refer to Figure 2.7). In the same manner as the braking torque does, the wheel load also influences the rotational dynamics of the wheel.

The only difference is that a changing wheel load has to be transferred into a changing braking force before it causes an angular acceleration of the wheel. Here a time delay appears: If an additional wheel load is applied, the tread elements of the tire have to deform first before the additional wheel load leads to an additional braking force. The time that it takes for this additional braking force to establish lies in the scale frame of a couple of milliseconds. In later chapters (refer to 5.5) this connection between wheel load and braking force is investigated. Similar thoughts hold true for the connection between a lowered wheel load and the decreasing braking force. In this direction the effect should establish faster. This assumption cannot be falsified by the results shown in Figure 5.5 on page 123, but it also cannot be verified, due to too high amounts of noise and deviations of wheel load.

But a thought experiment makes the direction of thinking clear: A drastic example for the influence which wheel load has on the rotational dynamics of a wheel is a completely lifted wheel. In this case no braking force can be applied at all and the wheel will be slowed down by a braking torque present very quickly. If the wheel is lifted, the braking force breaks down immediately. In the other direction, if the wheel is set back on the pavement again, it takes some amount of time for the tread elements to deform and to carry the braking force. This extreme example makes clear that the effect which a changing wheel load has on the braking force is assumably faster in the one direction than in the other.

The best thing in the sense of an optimal braking performance would be if each wheel was slowed down such that the braking slip is constant at the optimal braking slip for all times. This is because in this case $\mu = \mu(\lambda_{\mathrm{B,opt}}) = \mu_{\max}$ would be highest. If the wheel should be slowed down in such a way, this means that—assuming a constant deceleration of the vehicle—the angular acceleration of the wheel would have to be constant as well.

A constant angular acceleration of the wheel implies a constant torque acting on this wheel. That means the difference of braking torque and braking force times effective wheel radius needs to be constant, because those two quantities sum up to the total torque on the wheel. A fluctuation in braking torque should therefore always be compensated by a fluctuation of braking force in the other direction. This change in braking force can only be caused by a corresponding change in wheel load.

Furthermore, referring to section 2.2, the wheel load can provide yet another tool: By trying to increase wheel load at earlier times of the braking procedure and reducing it at later times, the braking force will also be increased at earlier times, which eventually leads to a shorter braking distance. Doing all these considerations it must always be kept in mind that the mean value of total wheel load with respect to time over a whole braking procedure can neither be in- nor decreased. It is always equal to the total static wheel load. For a single wheel of the front (rear) axle, the mean value over a braking procedure equals the static wheel load plus (minus) the wheel load due to the weight transfer from rear to front axle.

2.4 Conclusions

In this chapter the fundamentals of vehicle dynamics which are relevant for this thesis were introduced. The braking process in general and the possibilities to influence the braking force in particular were presented.

Concerning the braking procedure it was noticed that the braking distance can be reduced in two different ways:

- Increasing the time-average of the braking force
- Distributing braking force from later to earlier times of the braking procedure

The possibility to increase the time-averaged braking force is given by the fact that due to slip oscillations the maximum friction coefficient is not fully utilized in today's braking procedures.

Furthermore, besides the braking distance itself another measurand was introduced: The quality of the braking procedure, measured by means of the integral of the squared vehicle's velocity VI. This quantity indicates the possible damage in case a collision cannot be prevented anymore. The smaller VI, the better.

Depending on the distance of the center of mass and the pitching center, a braking procedure more or less leads to oscillations in the vertical tire force (the greater the distance, the more oscillations), even on an ideally even road. Those oscillations influence the braking behavior.

Two possible ways were introduced that are feasible to influence the braking distance: Either the control of braking torque or the control of wheel load. In this thesis the latter is investigated.

3 Tools and Research Environment

3.1 Active Shock-Absorbers

Shock absorbers in passenger car suspensions serve two different purposes: Firstly, they have to guarantee the passengers' riding comfort. Secondly, they have to care for a high handling performance. Both demands have in common that for their fulfillment it is necessary to reduce vibrations in the suspension system. This is done by dissipating energy in the shock absorbers.

For riding comfort purposes the focus lies on the vibrations of the vehicle's body, for an improved handling it lies on the oscillations of the vertical tire force—namely the wheel load. Shock absorbers as a part of the vehicle's suspension usually are mantled between wheel and body. They produce forces opposing the vibratory motion. Shock absorbers usually produce a higher damper force in rebound than in compression for the same damper velocity[1]. This is due to the fact that in compression the damper velocity can be much higher than in rebound, because if the vehicle is passing an obstacle that is similar to a step input, the wheel must be accelerated upwards very quickly in order to follow the step. The vehicle's body with its inertia standing against the damper force is also accelerated upwards. If the damping coefficient in compression was very large, the potentially very large damper velocity in compression would lead to a strongly accelerated vehicle body. This would bring unwanted oscillations into the system and could cause damages due to huge damper forces.

In the other direction, passing a step input with negative height or a hole, the damper velocity is only as large as the wheel is accelerated downwards by the spring force. There is no boundary restriction that implies that the wheel must be accelerated by a very high amount. Therefore, it does not do any harm if the damping coefficient is high in rebound. In fact, the rebound phase can be used to dissipate as much energy as possible. This is why the damping coefficient usually is approximately two times greater in rebound than in compression.

The same principle holds true in case of active shock absorbers. There, the rebound is harder than the compression stage (refer to Figure 4.3 on page 66), too. Active shock absorbers are characterized by the fact that their damping coefficients can be adjusted within a short amount of time. They do not only have one fixed characteristic line but rather—in case of continuously adjustable shock absorbers—an infinite number of characteristic lines. The two extreme characteristic lines shall be called 'hard' and 'soft' in this thesis (refer to Figure 4.12 on page 77).

The shock absorber that is used for all experimental testings is a so called CDC-shock absorber[2]. Its characteristic lines can be adjusted by an electromagnetic valve. The construction of this kind of shock absorber is shown in Figure 3.1. Here, via the opening

[1] Dixon (1999): The Shock Absorber Handbook p. 250.
[2] Continuous Damping Control by ZF Sachs AG

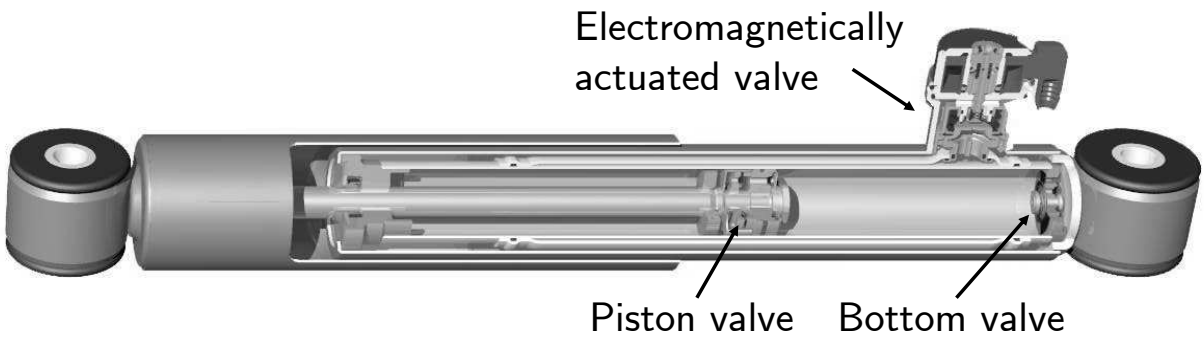

Figure 3.1: Example for an active shock absorber with external proportional and electromagnetically actuated valve. Source: ZF Sachs AG.

condition of an outlying electromagnetically actuated valve the damping ratio is changed. Constructions where the electromagnetically actuated valve is inside the shock absorber, integrated in the piston valve, are also known[3]. For the shock absorbers used in this thesis the hard damping is achieved by setting the current of the electromagnet to $I_{\mathrm{D}} = 0\,\mathrm{A}$. The soft damping is set by a damper current of $I_{\mathrm{D}} = 1.6\,\mathrm{A}$. Both characteristic lines (soft and hard) for the shock absorbers of the front and the rear axle can be seen in Figures 4.3 and 4.4 on pages 66 and 67. The reason for having the shock absorber in its hardest stage with no damper current present is that in case of a system failure the shock absorbers should not be soft but rather hard. This is because harder damping is supposably better in the sense of a higher handling performance and is therefore safer.

In Figure 3.2 the functional principle of active shock absorbers that are controlled by an electromagnetically actuated valve is shown. The two functional principles are an inlying active valve (A) and an outlying active valve (B). In case (A) the hydraulic oil that is pushed away by the piston rod in compression is pressed through the bottom valve into the intercepting chamber. At the same time the oil from below the active piston valve is pressed through this valve into the chamber above it. Both valves, bottom and active one, deliver part of the damping. In rebound, the oil streams back from the intercepting chamber into the piston chamber through the second bottom valve, whose damping factor can differ from the one of the bottom valve which is responsible for the damping in compression. Furthermore, the oil is pressed from the lower to the upper piston chamber through the active valve. In both stages (compression and rebound) part of the damping is delivered by the active valve. Thus, the damping coefficient can be influenced by changing the opening condition of this valve.

In case of an outlying active valve the same considerations hold true in general. The difference here is that the oil streams through the active valve always in the same direction. In compression, oil is passing through the piston and the active valve, in rebound, it is the bottom and the active valve which provide the damping.

For any shock absorber (no matter if active or not) the rebound/compression damping factor ratio s_{RC} shall be defined as the ratio between linearized damping coefficient in rebound and the linearized damping coefficient in compression:

$$s_{\mathrm{RC}} = \frac{k_{\mathrm{B,R}}}{k_{\mathrm{B,C}}} \tag{3.1}$$

[3] Causemann (2001): Kraftfahrzeugstoßdämpfer p. 60.

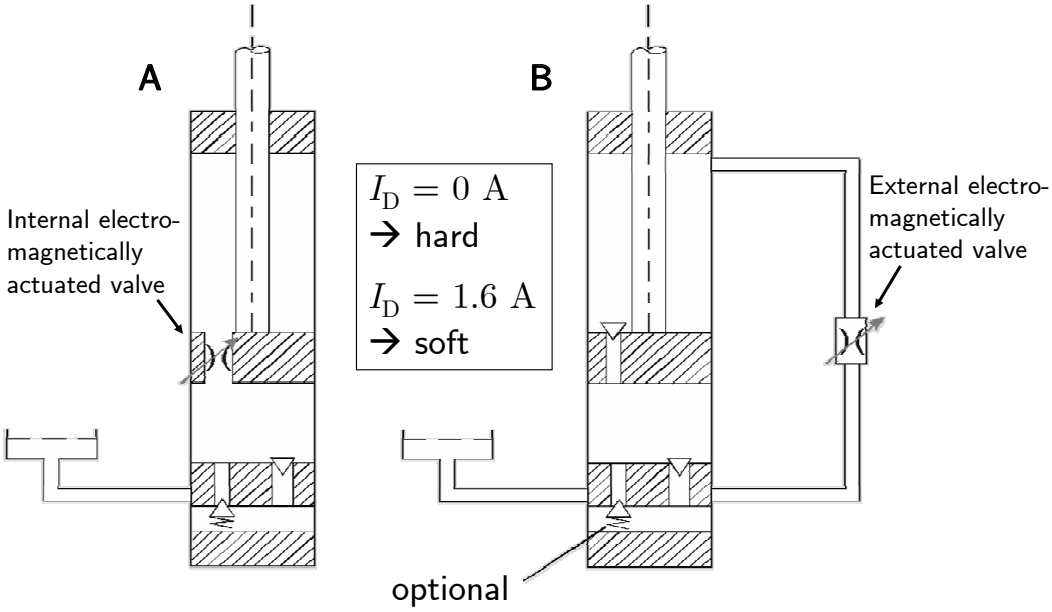

Figure 3.2: Principle of the function of active shock absorbers[4]. A: Internal electromagnetically actuated valve. B: External electromagnetically actuated valve.

For a passive shock absorber this factor is constant and—as already mentioned above—it usually has a value of approximately two. For active shock absorbers this ratio depends on the setting of the shock absorber for rebound and compression. If the shock absorber is set to hard in rebound and soft in compression, the ratio is largest. If it is set to soft in rebound and hard in compression, the ratio is smallest.

For an active shock absorber the spreading with respect to the characteristic lines for hard and soft damping s_{hs} shall be defined as the ratio between linearized damping coefficient in rebound or compression for hard damping and the linearized damping coefficient in rebound or compression for soft damping.

$$s_{\mathrm{hs,R}} = \frac{k^{\mathrm{h}}_{\mathrm{B,R}}}{k^{\mathrm{s}}_{\mathrm{B,R}}} \tag{3.2}$$

$$s_{\mathrm{hs,C}} = \frac{k^{\mathrm{h}}_{\mathrm{B,C}}}{k^{\mathrm{s}}_{\mathrm{B,C}}} \tag{3.3}$$

3.2 Testing Vehicle

The testing vehicle being used for all experimental investigations is an Opel Astra of the lastest generation, called Astra H. It is equipped with the so called Interactive Driving System-plus (IDS-plus), which includes Continuous Damping Control (CDC) by ZF Sachs AG, Germany. In series applications this semi-active suspension system mainly is controlled by a skyhook control algorithm which reduces the vertical oscillations of the body in order to improve the riding comfort. If a critical driving situation occurs, the control of this car's active shock absorbers is switched off, meaning that the dampers are

[4] Causemann (2001): Kraftfahrzeugstoßdämpfer p. 56

in their hardest possible setting. This means that during an ABS-braking—which is considered to be a critical situation—, the shock absorbers are not controlled and are therefore in the hard setting. Figure 3.3 shows the testing vehicle on the testing track 'Standard Road', which is an airfield that belongs to Technische Universität Darmstadt and is not in use for regular air traffic anymore.

Figure 3.3: The testing vehicle which is used for all experimental testings Opel Astra H 2.0i 16v Turbo on the testing track 'Standard Road'.

The IDS-plus system, besides the active shock absorbers, comes with several additional equipment that cannot be found in the standard series Astra without IDS-plus. These are namely five accelerometers to measure vertical wheel and body accelerations and an Electronic Control Unit (ECU) to handle the signals and calculate the damper current for each wheel individually. In Figure 3.4 the spring-and-shock-absorber unit of a front wheel of the testing vehicle is shown. The main components and their configuration in the car can be seen. The damper velocity is calculated from the signals of the accelerometers that provide the vertical wheel and body acceleration.

3.2.1 Testing Vehicle Specifications

The testing vehicle's specifications can be found in Table 3.1. The fact that the vehicle is a standard car that can be found in large numbers in the streets is important for the relevance and the transferability of the results gained from investigating the shock absorber controller.

3.2.2 Testing Vehicle Measurement System

Figure 3.5 shows the testing vehicle with its series configuration. Active shock absorbers are included in the series car as well as accelerometers at the front axle (wheels and body) and one accelerometer at the body above the rear axle. In the series application these sensors are connected to an Electronic Control Unit (ECU), which also includes the power amplifier for providing the damper current. The necessary damper current is calculated within the ECU for every wheel individually. It depends on the damper velocity v_{D}, which is calculated from the acceleration signals at the front axle and on the desired body movements (usually the control objective is to damp the body oscillations against a virtual

Table 3.1: Specifications of the testing vehicle. Sources: N.N. (2006c): Website – Opel Ireland, ZF Sachs AG, and own measuring. Own measuring are in bold.

Property	**Specification**
Make	Opel
Model	Astra 2.0i 16v Turbo
Engine capacity	$1998\,\mathrm{cm}^3$
Maximum power	$125\,\mathrm{kW}$ at $5{,}400\,\mathrm{min}^{-1}$
Maximum torque	$250\,\mathrm{Nm}$ at $1{,}950\,\mathrm{min}^{-1}$
Gross vehicle weight (fl+fr+rl+rr)	$\mathbf{1{,}700\,kg = 2 \cdot 480\,kg + 2 \cdot 370\,kg}$ (fueled, including measurement equipment, driver and one passenger)
Front suspension	McPherson struts, Anti-roll bar, Sub frame, Hydraulic bushings $i_{\mathrm{D,f}} = \mathbf{1}$ $i_{\mathrm{S,f}} = \mathbf{1}$ $\varepsilon_{\mathrm{f}} = 3.5°$
Rear suspension	Torsion beam, Displaced shock absorbers and coil springs $i_{\mathrm{D,r}} = \mathbf{0.68}$ $i_{\mathrm{S,r}} = \mathbf{0.88}$ $\varepsilon_{\mathrm{r}} = 26°$
Shock Absorbers	Interactive Driving System-plus (IDS-plus) with Continuous Damping Control (CDC)
Tires	Pirelli P6000, 205/55 R16 91W $r_{\mathrm{eff}} = \mathbf{0.304...0.307\,m}$ Standard inflation pressure $p_{\mathrm{T}} = \mathbf{2.3\,bar}$
Mass moments of inertia	$J_{\mathrm{W,f}} = \begin{cases} \mathbf{1.3\,kg\,m^2 \pm 0.1\,kg\,m^2} & for \text{ neutral position} \\ \mathbf{3.1\,kg\,m^2 \pm 0.1\,kg\,m^2} & for \text{ third gear} \\ \mathbf{6.3\,kg\,m^2 \pm 0.2\,kg\,m^2} & for \text{ second gear} \end{cases}$ $J_{\mathrm{W,r}} = \mathbf{0.95\,kg\,m^2 \pm 0.08\,kg\,m^2}$ $J_{\mathrm{B}} = 1870\,\mathrm{kg\,m}^2$
Rims	Steel rims, 6.5"x16" ET 37
Transmission	Front-wheel drive Six-speed manual gearbox
Braking system	Front ventilated disk brakes (280 mm diameter) Rear disc brakes (264 mm diameter) Friction factor between braking pads and braking disc $\mu_{\mathrm{PD}} \approx 0.4$ Factor to transfer braking pressure into braking torque front $i_{p_{\mathrm{B}}2M_{\mathrm{B}},\mathrm{f}} \approx 24\,\mathrm{Nm/bar}$ Factor to transfer braking pressure into braking torque rear $i_{p_{\mathrm{B}}2M_{\mathrm{B}},\mathrm{r}} \approx 10\,\mathrm{Nm/bar}$ Anti-lock Braking System (ABS) with Electronic Brake Force Distribution (EBD) Gradient with which braking pressure is relieved by the ABS $\dot{p}_{\mathrm{B,rel}} = \mathbf{-1{,}000\,bar/s}$ Gradient with which braking pressure is increased by the ABS $\dot{p}_{\mathrm{B,inc}} = \mathbf{+250\,bar/s}$
Dimensions	Wheel base $l = 2.614\,\mathrm{m}$ Distance from front axle to center of gravity $l_{\mathrm{f}} = \mathbf{1.13\,m}$ Distance from rear axle to center of gravity $l_{\mathrm{r}} = \mathbf{1.48\,m}$ Height of center of gravity $h_{\mathrm{CG}} = \mathbf{0.52\,m}$

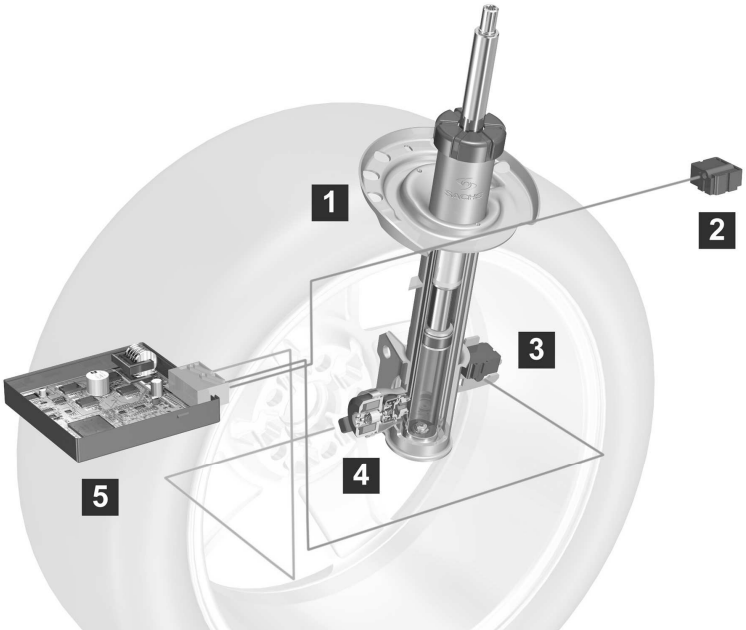

Figure 3.4: Spring-and-shock-absorber unit of a front wheel of the testing vehicle. 1: CDC-shock absorber, 2: Accelerometer for vertical body accelerations, 3: Accelerometer for vertical wheel accelerations, 4: Electromagnetically actuated valve, 5: Electronic Control Unit (ECU). Source: ZF Friedrichshafen AG.

sky-hook). The focus is put on the front axle (it is only there that wheel accelerometers are applied in series application), because the front axle supports 57 % of the total wheel load and for series applications it can furthermore be assumed that the vertical excitation at the rear axle will with a phase shift which is reciprocal to the vehicle's speed be the same as at the front axle.

The standard components of the series vehicle are extended by several additional measuring equipment and by an active element, a braking machine. Table 3.2 gives on overview of the measuring equipment.

The measurement system used in the testing vehicle uses analog as well as digital signals. All quantities which are relevant for a braking procedure and which are vehicle internal quantities can be measured. An external quantity e. g. would be the friction coefficient between pavement and tire. This one cannot be measured with the measurement system presented. The core of the measuring and controlling system is a dSpace Autobox which measures all signals, calculates the optimal damper current, and gives this as an output to the active shock absorbers. All data is gained with a sampling rate of $f_s = 2,000$ Hz, in order to be able to measure effects that take place in the time frame of milliseconds.

All quantities measured can be divided into two subsections: First, those measurands that are measured to objectively value the braking procedure and to monitor the parameters that influence the braking distance. These sensor signals are not used to actually influence the braking distance by using them as inputs for a controller, but they are rather stored to be treated off-line, after the test drive is finished. For those measurands it is not critical if their signal is slightly noisy or if there is an offset. Noise and offsets usually

[5] The accelerometers of the body have an integrated high-pass filter of first order with a cutting frequency of 0.5 Hz.

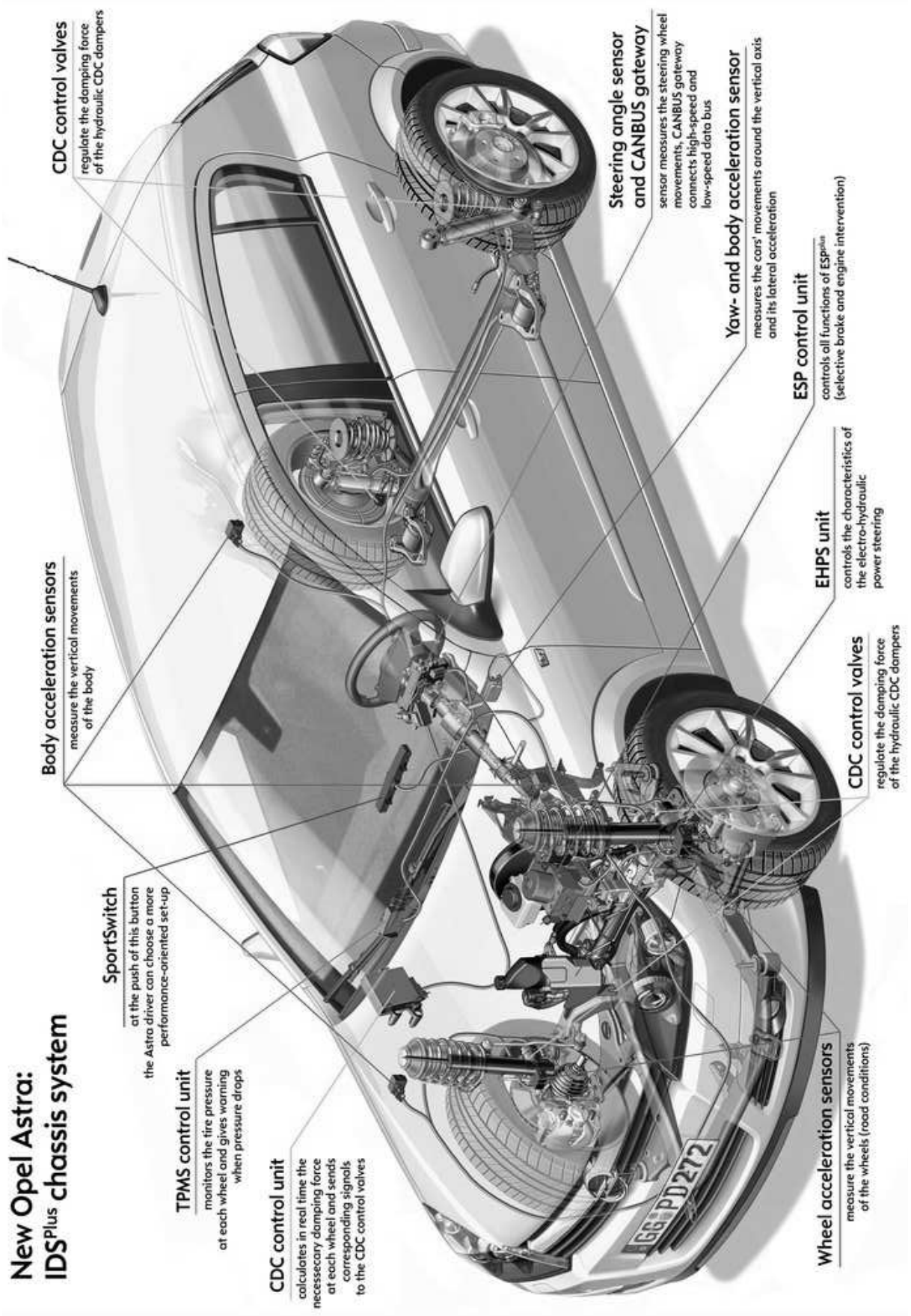

Figure 3.5: The testing vehicle with its series equipment. Source: N.N. (2006a): Website – all4engineers.

Table 3.2: Sensors and actuators in the testing vehicle

Physical Quantity	**Sensor**	**Position**	**DP**
Pressure	Piezo-electric sensor	Wheel braking cylinder fl, fr, rl, rr, and main braking cylinder	analog
Opening condition of ABS-valves	Digital information from the ECU of the ABS	Wheel fl, fr, rl, rr	binary
Displacement	ASM position sensor, potentiometer	Wheel to body fl, fr, rl, and rr	analog
Velocity	Datron Correvit, optical sensor	Rear bumper, longitudinal	analog
Angular velocity	Series sensors	Wheel fl, fr, rl, and rr	CAN
Acceleration	Piezo-electric sensor, same sensor-model as used in the production-model of the Opel Astra[5]	Wheel fl, fr, rl, and rr, vertical, Body fl, fr, rl, and rr, vertical at suspension strut mounting, Body, longitudinal	analog
Force and torque	Kistler 6-components measuring rim, piezo-electric	Wheel load fl, braking force fl, and braking torque fl	analog
Temperature	Thermocouple Typ K	Brake disc fl	analog
Light intensity	Light barrier sensor	Rear bumper	analog
	Actuator	**Position**	**DP**
	Braking machine, electric motor	Attached to the braking pedal	analog
	Magnetic coils	Active shock absorbers fl, fr, rl, and rr	CAN

can be handled off-line with a minimum of loss in signal accuracy. As for the noise, this is because the relevant frequencies lie way below the typical noise frequencies in automotive applications (20–30 Hz compared to 100 Hz and more).

The other group of measurands are more crucial with respect to their realtime computability. It is those measurands which deliver the inputs for the controller—that is why they need to be computed in realtime while driving and braking. The vertical accelerometers provide the signals from which the dynamic wheel load is computed, the position sensors provide the signals from which the damper velocity is determined. Thus, for the vertical accelerations an offset correction is undertaken at the beginning of every test day.

For the position sensors the offset can be neglected, because the damper velocity is the derivative of their signals, and a possible offset therefore does not play a role in the calculation of the desired signal. But by taking the derivative, high-frequency noise is amplified. Hence, filtering is necessary for this signal, which leads to a phase shift. Since the relevant frequencies in the signal of the damper velocity are much lower than the necessary cutting frequency (refer to 5.9 on page 132 for the frequencies of the damper velocity during full-braking, the cutting frequency lies at 40 Hz), this phase shift influences the course of damper velocity in a time frame of a couple of milliseconds. Though there is this additional time delay on top of all other time delays, this one is small compared to the others.

Another crucial sensor whose signal needs to be present in realtime is the light barrier attached to the rear bumper. With this sensor not only the braking procedure is initiated, but also the determination of the longitudinal velocity is verified for every test drive. It is for every test drive that five meters before the light barrier reflector whose signal initiates the braking procedure another light barrier reflector is placed. Thus, knowing this distance of five meters during which the velocity of the vehicle is still constant, the signal from the so called Correvit sensor can be verified and, if necessary, calibrated.

3.2.3 Measuring Rim

A 6-component measuring rim is used for test drives on defined obstacles to determine the wheel load and the braking force at the front left wheel (refer to section 5.2.2 for these test drives). A wheel of the front axle is chosen to mount the measuring rim at, because the front axle is responsible for more than 3/4 of the overall braking force.

Figure 3.6 shows this measuring rim installed at the front left wheel of the testing vehicle. The actual measuring element is connected with the rim well via two rigid adapters. The purpose of using the measuring rim is to measure the wheel load—the vertical tire force in the contact zone of tire and pavement. But between the measurand 'real wheel load' F_z and the place of measuring, where the force $F_{z,rim}$ is captured, lies the tire, which cannot be treated as a rigid body. Thus, $F_{z,rim}$ only represents F_z with high precision at frequencies that are such low or such high that the tire can be assumed to be rigid. Evers and Reichel investigated this topic in detail for a measuring rim mounted to a 1999 BMW 5 series passenger car on a 4-post test rig[6].

Figure 3.7 shows the transfer function from the force that is measured by the test rig described in section 3.3 and that is representing F_z in high precision to the force $F_{z,rim}$

[6] Evers et al. (2002): Radkraft-Dynamometer (RWD/FWD) als Entwicklungswerkzeug für Felge und Radaufhängung.